Singularity in the electron-core potential as a gateway to accurate multielectron ionization spectra in strongly driven atoms

A. Emmanouilidou, M. B. Peters ⬡, and G. P. Katsoulis

Department of Physics and Astronomy, University College London, Gower Street, London WC1E 6BT, United Kingdom

We demonstrate a general three-dimensional semiclassical model as a powerful technique for the study of correlated multielectron escape in atoms driven by infrared laser pulses at intensities where electron-electron correlation prevails. We do so in the context of triple ionization of strongly driven Ne. Our model fully accounts for the singularity in the Coulomb potentials of a recolliding electron with the core and a bound electron with the core as well as for the interaction of a recolliding with a bound electron. To avoid artificial autoionization, our model employs effective potentials to treat the interaction between bound electrons. We show the accuracy of our model by obtaining triple ionization distributions of the sum of the final electron momenta which we find to be in very good agreement with experiments. Also, we explain the main features of these momenta distributions in terms of the prevalent pathways of correlated three-electron escape in Ne. We also show that the different ionization pathways prevailing in three-electron escape in strongly driven Ne versus Ar give rise to different momenta distributions in these two atoms. Our general model may be used to identify novel ultrafast phenomena and to motivate further experiments in strong field science.

In atoms driven by intense and infrared laser pulses, nonsequential multielectron ionization (NSMI) is a fundamental process governed by electron-electron correlation [1]. Recollisions govern nonsequential multielectron ionization. During a recollision an electron tunnels out through the field-lowered Coulomb barrier, moves into the laser field, and can then return to the core to recollide and transfer energy to the other electrons [2]. Besides the tunneling step, the other steps in the three-step model can be described classically [2]. While nonsequential double ionization (NSDI) has been studied extensively both theoretically and experimentally [3,4], three-dimensional (3D) quantum-mechanical studies still remain quite challenging [5–7]. For nonsequential triple ionization (NSTI), only few theoretical studies exist, mostly formulated in the dipole approximation. For NSTI, most studies employ lower dimensionality classical [8,9] and quantum-mechanical [10,11] models to reduce the complexity and computational resources required. However, lower dimensionality results in a nonaccurate description of the electron-electron interaction during triple ionization. Currently, only classical or semiclassical 3D models of NSTI are available [9,12–15]. Here, we argue that the main disadvantage of available classical and quantum models of NSTI is their softening of the interaction of each electron with the core. This results in ionization spectra that differ from experimental ones obtained, for instance, for driven Ne and Ar [16–22].

Concerning NSTI, for quantum-mechanical models, softening the Coulomb potential of each electron with the core affords a computationally tractable problem. For classical and semiclassical models, the reason is fundamental and concerns unphysical autoionization. Classically there is no lower-energy bound. Hence, when a bound electron undergoes a close encounter with the core, the singularity in the Coulomb potential allows this electron to acquire a very negative energy. This can lead to the artificial escape of another bound electron through the Coulomb interaction between bound electrons. To avoid this, most classical and semiclassical models of NSTI soften the Coulomb potential [9,12,13] or add Heisenberg potentials [23] (effective softening) to mimic the Heisenberg uncertainty principle and prevent each electron from a close encounter with the core [14,15].

However, softening the Coulomb potential fails to accurately describe electron scattering from the core [24,25]. Indeed, the ratio of the scattering amplitude for the soft-core potential over the one for the Coulomb potential decreases exponentially with increasing momentum transfer [24,25]. For recollisions [2], this implies that soft potentials are quite inaccurate for high-energy recolliding electrons that backscatter. Hence, it is no surprise that classical models that include the singularity in the Coulomb electron-core potential result in accurate double ionization spectra. Indeed, with a classical model for driven two-electron atoms [26], the predecessor of the model of NSMI discussed here, we have shown that backscattering of the recolliding electron from the core gives rise to the fingerlike structure in the two electron correlated momenta of driven He [5,27,28]. We have also obtained double ionization spectra in very good agreement with an *ab initio* quantum-mechanical calculation for driven He [29] and with an experiment for Ar driven by near-single

cycle laser pulses [30]. We have also identified the striking slingshot-NSDI mechanism where the exact treatment of the electron-core interaction is of paramount importance [31].

Here, we provide a general 3D classical model of NSMI developed in the nondipole framework. The main premise in our model is that two interactions are most important during a recollision and hence are treated exactly. Motivated by the above-mentioned studies [24–26,30,31], we account for the singularity in the Coulomb potential between each electron, bound or quasifree, and the core. Quasifree refers to a recolliding electron or an electron escaping to the continuum. Also, the Coulomb potential between each pair of a quasifree and a bound electron and hence the transfer of energy from a quasifree to a bound electron is treated exactly. Using this model, for nonsequential triple ionization of strongly driven Ne, we obtain triple ionization spectra in excellent agreement with experiment [17].

Accounting for the singularity in electron-core interactions can lead to unphysical autoionization through energy transfer between bound electrons. To avoid this, we use effective Coulomb potentials to account for the interaction of a bound-bound electron pair (referred to as ECBB—effective Coulomb potential for bound-bound electrons). That is, we approximate the energy transfer from a bound to a bound electron. Hence, we expect that the ECBB model will be more accurate for laser pulse parameters where multielectron ionization due to the transfer of energy between electrons in excited states after recollisions plays less of a role. A sophisticated aspect of the ECBB model involves deciding during time propagation whether an electron is quasifree or bound. That is, we decide on the fly if the full or effective Coulomb potential describes the interaction between a pair of electrons. To do so, we use a set of simple criteria detailed below.

We demonstrate the accuracy of the ECBB model in the context of correlated three-electron escape in strongly driven Ne. We show that the z component of the sum of the final electron momenta has excellent agreement with experiment [17]. Here, the electric field is linearly polarized along the z axis. The ECBB model has been previously used to study triple ionization of strongly driven Ar [32]. However, the striking agreement with experiment for strongly driven Ne unveils the ECBB model as a powerful technique for studying correlated multielectron ionization in driven atoms. Moreover, we interpret the features of the z component of the sum of the final electron momenta in terms of the main recollision pathways for driven Ne and Ar. The differences in the ionization spectra of the two atoms are found to be due to direct pathways prevailing triple ionization of Ne.

We employ the ECBB model [32] to compute triple and double ionization observables of driven Ne. In what follows, TI refers to nonsequential triple ionization (NSTI) and DI to nonsequential double ionization (NSDI). One electron tunnel ionizes through the field-lowered Coulomb barrier at time t_0. In our previous studies of double ionization [26,31,33,34] tunneling occurs with a rate described by the quantum-mechanical Ammosov-Delone-Krainov formula [35,36]. Here, using the same formula, hence the term semiclassical model, we obtain a rate that also accounts for depletion of the initial ground state (see Supplemental Material [37]). We find t_0, using importance sampling [38] in the time interval $[-2\tau, 2\tau]$ where the electric field is nonzero; τ is the full width at half maximum of the pulse duration in intensity. The exit point of the recolliding electron along the direction of the electric field is obtained analytically using parabolic coordinates [39]. The electron momentum along the electric field is set equal to zero, while the transverse one is given by a Gaussian distribution [36,40,41]. For the initially bound electrons, we employ a microcanonical distribution [32].

In the ECBB model, we fully account for the magnetic field of the laser pulse, i.e., the magnetic field component of the Lorentz force, as well as the motion of the core and the three electrons. The four-body Hamiltonian is

$$H = \sum_{i=1}^{4} \frac{[\tilde{\mathbf{p}}_i - Q_i \mathbf{A}(y,t)]^2}{2m_i} + \sum_{i=2}^{4} \frac{Q_i Q_1}{|\mathbf{r}_1 - \mathbf{r}_i|} + \sum_{i=2}^{3}\sum_{j=i+1}^{4} [1 - c_{i,j}(t)] \frac{Q_i Q_j}{|\mathbf{r}_i - \mathbf{r}_j|} + \sum_{i=2}^{3}\sum_{j=i+1}^{4} c_{i,j}(t)$$
$$\times \{V_{\text{eff}}[\zeta_j(t), |\mathbf{r}_1 - \mathbf{r}_i|] + V_{\text{eff}}[\zeta_i(t), |\mathbf{r}_1 - \mathbf{r}_j|]\}, \tag{1}$$

where Q_i is the charge, m_i is the mass, $\mathbf{r}_i$ is the position vector, and $\tilde{\mathbf{p}}_i$ is the canonical momentum vector of particle i. The mechanical momentum $\mathbf{p}_i$ is given by

$$\mathbf{p}_i = \tilde{\mathbf{p}}_i - Q_i \mathbf{A}(y,t). \tag{2}$$

The effective Coulomb potential that an electron i experiences at a distance $|\mathbf{r}_1 - \mathbf{r}_i|$ from the core (particle 1 with $Q_1 = 3$), due to the charge distribution of electron j is equal to

$$V_{\text{eff}}(\zeta_j, |\mathbf{r}_1 - \mathbf{r}_i|) = \frac{1 - (1 + \zeta_j|\mathbf{r}_1 - \mathbf{r}_i|)e^{-2\zeta_j|\mathbf{r}_1 - \mathbf{r}_i|}}{|\mathbf{r}_1 - \mathbf{r}_i|}, \tag{3}$$

with ζ_j the effective charge of particle j [32,42]. When $\mathbf{r}_i \to \mathbf{r}_1$, the effective potential is equal to ζ_j. This ensures a finite transfer of energy between bound electrons i and j and hence that no artificial autoionization occurs. The functions

$c_{i,j}(t)$ determine at time t during propagation whether the full Coulomb or effective $V_{\text{eff}}(\zeta_i, |\mathbf{r}_1 - \mathbf{r}_j|)$ and $V_{\text{eff}}(\zeta_j, |\mathbf{r}_1 - \mathbf{r}_i|)$ potentials describe the interaction between electrons i and j [32]. The effective potentials are activated only when both electrons are bound.

We determine on the fly whether an electron is quasifree or bound using the following simple criteria. A quasifree electron can transition to bound following a recollision. Specifically, once the quasifree electron has its closest encounter with the core, this electron transitions to bound if its position along the z axis is influenced more by the core than the electric field. Also, a bound electron transitions to quasifree due to the transfer of energy during a recollision or from the laser field. In the former case, this transition occurs if the potential energy of this bound electron with the core

is constantly decreasing. In the latter case, if the energy of the bound electron becomes positive and remains positive, it transitions to quasifree. The criteria are discussed in detail and illustrated in the Supplemental Material [37].

Details of how we accurately account for the Coulomb singularity and the leapfrog technique we employ to solve Hamilton's equations of motion are given in Ref. [32]. We stop the propagation when the energy of each particle converges. We label the trajectory as triply or doubly ionized if three or two electrons have positive energy, and compute the TI and DI probabilities out of all events.

We use a vector potential of the form

$$\mathbf{A}(y,t) = -\frac{E_0}{\omega} \exp\left[-2\ln(2)\left(\frac{ct-y}{c\tau}\right)^2 \right] \sin(\omega t - ky)\hat{\mathbf{z}},$$

(4)

where $k = \omega/c$ is the wave number of the laser field. The direction of the vector potential and the electric field, $\mathbf{E}(y,t) = -\frac{\partial \mathbf{A}(y,t)}{\partial t}$, is along the z axis, while the direction of light propagation is along the y axis. The magnetic field, $\mathbf{B}(y,t) = \nabla \times \mathbf{A}(y,t)$, points along the x axis. The pulse duration is $\tau = 25$ fs, while the wavelength is 800 nm. For Ne, we consider intensities 1.0, 1.3, and 1.6 PW/cm^2. For Ar, previously studied in Ref. [32], we consider only 0.4 PW/cm^2. The highest intensities considered here, 1.6 PW/cm^2 for Ne and 0.4 PW/cm^2 for Ar, are chosen such that the probability for a second electron to tunnel ionize solely due to the laser field is very small [37]. Hence, electron-electron correlation prevails in TI and DI, with the bound electrons ionizing only due to recollisions. The smaller intensity for Ar is consistent with its smaller first ionization potential.

Here, we compare the results obtained with the ECBB model both with experiment and with the semiclassical 3D model that employs Heisenberg potentials (H model) (see Supplemental Material [37]). This potential depends on a parameter α, with a large value restricting more the phase space an electron can access around the core [32,37]. Hence, the H model results in an effective softening of the electron-core potential. We do not compare with classical models that explicitly soften the Coulomb potential. The reason is that a previous study of NSDI in Ar [43] has shown that the H model and the model that includes the Coulomb singularity [26,29,30] better agree with experiment.

In Fig. 1, for driven Ne, we compute the ratio of double to triple ionization probability and compare with experiment [17] and the H model. For all three intensities, we find the probability ratio $P_{\mathrm{DI}}/P_{\mathrm{TI}}$ obtained with the ECBB model (black circles) to be consistently close to experiment (gray squares). In contrast, the H model for $\alpha = 2$ and $\alpha = 4$ does not agree with experiment for 1.0 and 1.3 PW/cm^2. Also, we find that the DI probability depends on the value of α for driven Ne [37], similar to our previous findings for driven Ar [32].

Next, we compute the TI probability distribution of the z component of the sum of the final electron momenta, sum of p_z (see the black lines in Fig. 2). We compare with measurements (gray lines) [17], smoothed in Fig. 2, and with the H model for $\alpha = 2$ (green lines). We find the ECBB distributions to be doubly peaked at all intensities. With increasing
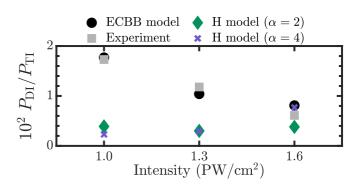

FIG. 1. For Ne, the ratio of DI to TI probability obtained with the ECBB model (black circles), the H model, and experiment (gray squares) [17].

intensity, the peaks become less pronounced with an increasing probability for the sum of p_z to be around zero. These features agree well with experiment. Also, the ECBB distributions peak at roughly the same values of the sum of the electron momenta as the experiment. This excellent agreement further illustrates the accuracy of the ECBB model. In contrast, the H model distributions have a significantly higher probability for the sum of the final electron momenta to be around zero. Also, they are less wide compared to the ECBB model and experimental distributions. The difference is more pronounced at 1.6 PW/cm^2 [Fig. 2(c)], with the H model distribution peaking around zero and the other two distributions being doubly peaked. This difference shows that in the H model the effective softening of the interaction of the recolliding electron with the core results in electrons escaping with lower energy. This gives rise to less wide distributions that have a significant probability for the sum of p_z to be around zero.

Next, using the ECBB model, we analyze the TI events and identify the recollision pathways that prevail in the three-electron escape of driven Ne. In the Supplemental Material [37], we outline the algorithm we use to identify the recollision pathways. An electron is deemed as ionizing soon after recollision if the difference between the recollision time and the ionization time is less than $t_{\mathrm{diff}} = T/8$, where T is the period of the laser pulse. During this time interval, the interpotential energy between the recolliding and a bound electron
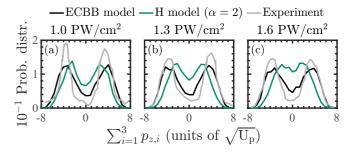

FIG. 2. For Ne, TI probability distributions of the sum of p_z obtained with the ECBB model (black lines), with the H model (green lines), and measured experimentally [17] (gray lines). Distributions are normalized to one. U_p is the ponderomotive energy equal to $E_0^2/4\omega^2$.
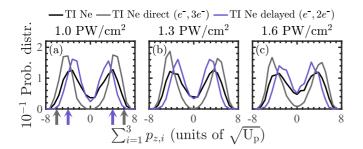
FIG. 3. For Ne, probability distributions of the sum of p_z for TI obtained with the ECBB model for all (black), direct (dark gray), and delayed (blue) events.
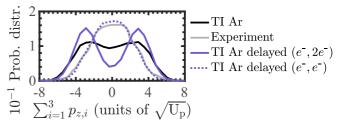

FIG. 4. For Ar, probability distributions of the sum of p_z for TI obtained experimentally [20] (gray) and with the ECBB model for all (black) and delayed $(e^-, 2e^-)$ (blue) and delayed (e^-, e^-) events (blue dotted).

undergoes a sharp change. The recollision time is identified from the maxima in the interpotential energies between the recolliding and each of the bound electrons [37]. The ionization time of electron i is defined as the time when the compensated energy $\{[\mathbf{p}_i - \mathbf{A}(y, t)]^2 + V(r_i)\}$ of this electron becomes positive and remains positive thereafter [44].

For driven Ne, we find that two are the main recollision pathways contributing to triple ionization, the direct $(e^-, 3e^-)$ and the delayed $(e^-, 2e^-)$. For a recollision to take place, an electron tunnels out through the field-lowered Coulomb barrier [2]. This electron can then return to the parent ion to recollide and transfer energy to the remaining electrons. In the direct pathway, all three electrons ionize soon after recollision, i.e., there are three highly correlated electron pairs. In the delayed $(e^-, 2e^-)$ pathway, the recolliding electron transfers enough energy for only two electrons to ionize soon after recollision, while the other electron ionizes with a delay. Hence, there is only one highly correlated electron pair. At all three intensities, we find that recollisions occur around a zero of the electric field and a maximum of the vector potential, resulting in a large final electron momentum with magnitude $E_0/\omega = 2\sqrt{U_p}$. In the direct pathway, all three electrons escape with large momenta p_z versus two electrons in the delayed $(e^-, 2e^-)$ pathway (see also the correlated electron momenta in the Supplemental Material [37]).

Next, we explain the features of the distribution of the sum of p_z for all TI events, both the experimental and the ECBB model ones (Fig. 2), in terms of the direct and delayed $(e^-, 2e^-)$ pathways. In Fig. 3, for all three intensities, we show that the distribution of the sum of p_z extends up to roughly $\pm 3 \times 2\sqrt{U_p}$ for the direct pathway [gray arrows in Fig. 3(a)] and up to $\pm 2 \times 2\sqrt{U_p}$ for the delayed $(e^-, 2e^-)$ pathway [blue arrows in Fig. 3(a)]. This is due to three electrons in the direct and two electrons in the delayed pathway escaping with large momentum $2\sqrt{U_p}$. This is consistent with the distribution of the sum of p_z for all TI events extending up to $\pm\beta \times 2\sqrt{U_p}$, with $2 < \beta < 3$. Also, for both pathways, the distributions are doubly peaked, giving rise to the double peaks of the distribution of the sum of p_z for all TI events. Moreover, in the direct pathway the distribution is roughly zero around the sum of p_z being zero. In contrast, in the delayed pathway, with increasing intensity, the peaks become less pronounced with an increasing probability for the sum of p_z to be around zero. Hence, this feature observed in the distribution of the sum of p_z for all TI events (Fig. 2) is due to the delayed pathway. For the H model, we find the direct

one to be a minor pathway, while the delayed $(e^-, 2e^-)$ one contributes the most to TI. This is consistent with soft potentials not accurately describing the scattering of a recolliding electron from the core [24].

Finally, for Ar, we find that the delayed $(e^-, 2e^-)$ and (e^-, e^-) pathways prevail at 0.4 PW/cm^2. In the latter pathway, the recolliding electron has enough energy to ionize only one electron soon after recollision. In the (e^-, e^-) pathway electrons escape with very small momenta (see correlated electron momenta in the Supplemental Material [37]). The contribution of these pathways to the distribution of the sum of p_z for all TI events is shown in Fig. 4. As for TI of Ne, for Ar, the distribution of the sum of p_z corresponding to the $(e^-, 2e^-)$ pathway is doubly peaked with a nonzero value around the sum of p_z being zero (blue line in Fig. 4). The distribution corresponding to the (e^-, e^-) pathway (blue dotted line in Fig. 4) peaks around the sum of p_z being zero. Interestingly, this distribution of the delayed (e^-, e^-) pathway is in very good agreement with the experimental distribution (gray line) at 0.3 PW/cm^2, with no measurements available at 0.4 PW/cm^2. The ECBB model distribution is more wide compared to the experimental one but also has a significant value around the sum of p_z being zero. Hence, for Ar, the ECBB model overestimates the contribution of the more correlated $(e^-, 2e^-)$ versus the less correlated (e^-, e^-) delayed pathway. Given the above, it is clear that three-electron escape is significantly less correlated in Ar than Ne.

In conclusion, we demonstrate that the ECBB 3D semiclassical model is a powerful tool to study correlated multielectron escape in driven atoms. To do so, we study three-electron ionization in Ne driven by infrared pulses. We show that the triple ionization probability distribution of the sum of the final electron momenta obtained with the ECBB model is in very good agreement with experiments. This agreement supports the premise of the ECBB model. That is, to obtain accurate multielectron ionization spectra it is important during a recollision to accurately account for the interaction between the recolliding and the bound electron and for the interactions of the bound and recolliding electron with the core. The ECBB model is developed in a general framework and can thus be easily extended to address the correlated escape of more than three electrons in driven atoms. It can also be extended to address driven molecules. We expect the ECBB model will be employed to study problems currently out of reach, leading to identifying novel ultrafast phenomena and to motivating additional experiments in strong field science.

[1] A. l'Huillier, L. A. Lompre, G. Mainfray, and C. Manus, Phys. Rev. A **27**, 2503 (1983).

[2] P. B. Corkum, Phys. Rev. Lett. **71**, 1994 (1993).

[3] W. Becker and H. Rottke, Contemp. Phys. **49**, 199 (2008).

[4] F. Krausz and M. Ivanov, Rev. Mod. Phys. **81**, 163 (2009).

[5] J. S. Parker, B. J. S. Doherty, K. T. Taylor, K. D. Schultz, C. I. Blaga, and L. F. DiMauro, Phys. Rev. Lett. **96**, 133001 (2006).

[6] A. Zielinski, V. P. Majety, and A. Scrinzi, Phys. Rev. A **93**, 023406 (2016).

[7] J. Zhu and A. Scrinzi, Phys. Rev. A **101**, 063407 (2020).

[8] K. Sacha and B. Eckhardt, Phys. Rev. A **64**, 053401 (2001).

[9] P. J. Ho and J. H. Eberly, Phys. Rev. Lett. **97**, 083001 (2006).

[10] J. H. Thiede, B. Eckhardt, D. K. Efimov, J. S. Prauzner-Bechcicki, and J. Zakrzewski, Phys. Rev. A **98**, 031401(R) (2018).

[11] D. K. Efimov, A. Maksymov, M. Ciappina, J. S. Prauzner-Bechcicki, M. Lewenstein, and J. Zakrzewski, Opt. Express **29**, 26526 (2021).

[12] Y. Zhou, Q. Liao, and P. Lu, Opt. Express **18**, 16025 (2010).

[13] Q. Tang, C. Huang, Y. Zhou, and P. Lu, Opt. Express **21**, 21433 (2013).

[14] H. Jiang and F. He, Phys. Rev. A **104**, 023113 (2021).

[15] H. Jiang, D. Efimov, F. He, and J. S. Prauzner-Bechcicki, Phys. Rev. A **105**, 053119 (2022).

[16] R. Moshammer, B. Feuerstein, W. Schmitt, A. Dorn, C. D. Schröter, J. Ullrich, H. Rottke, C. Trump, M. Wittmann, G. Korn, K. Hoffmann, and W. Sandner, Phys. Rev. Lett. **84**, 447 (2000).

[17] A. Rudenko, T. Ergler, K. Zrost, B. Feuerstein, V. L. B. de Jesus, C. D. Schröter, R. Moshammer, and J. Ullrich, J. Phys. B: At., Mol. Opt. Phys. **41**, 081006 (2008).

[18] N. Ekanayake, S. Luo, B. L. Wen, L. E. Howard, S. J. Wells, M. Videtto, C. Mancuso, T. Stanev, Z. Condon, S. LeMar, A. D. Camilo, R. Toth, W. B. Crosby, P. D. Grugan, M. F. Decamp, and B. C. Walker, Phys. Rev. A **86**, 043402 (2012).

[19] O. Herrwerth, A. Rudenko, M. Kremer, V. L. B. de Jesus, B. Fischer, G. Gademann, K. Simeonidis, A. Achtelik, T. Ergler, B. Feuerstein, C. D. Schröter, R. Moshammer, and J. Ullrich, New J. Phys. **10**, 025007 (2008).

[20] K. Zrost, A. Rudenko, T. Ergler, B. Feuerstein, V. L. B. de Jesus, C. D. Schröter, R. Moshammer, and J. Ullrich, J. Phys. B: At., Mol. Opt. Phys. **39**, S371 (2006).

[21] A. Rudenko, K. Zrost, B. Feuerstein, V. L. B. de Jesus, C. D. Schröter, R. Moshammer, and J. Ullrich, Phys. Rev. Lett. **93**, 253001 (2004).

[22] H. Shimada, Y. Nakai, H. Oyama, K. Ando, T. Kambara, A. Hatakeyama, and Y. Yamazaki, Nucl. Instrum. Methods Phys. Res., Sect. B **235**, 221 (2005).

[23] C. L. Kirschbaum and L. Wilets, Phys. Rev. A **21**, 834 (1980).

[24] R. R. Pandit, V. R. Becker, K. Barrington, J. Thurston, L. Ramunno, and E. Ackad, Phys. Plasmas **25**, 043302 (2018).

[25] R. R. Pandit, Y. Sentoku, V. R. Becker, K. Barrington, J. Thurston, J. Cheatham, L. Ramunno, and E. Ackad, Phys. Plasmas **24**, 073303 (2017).

[26] A. Emmanouilidou, Phys. Rev. A **78**, 023411 (2008).

[27] A. Staudte, C. Ruiz, M. Schöffler, S. Schössler, D. Zeidler, T. Weber, M. Meckel, D. M. Villeneuve, P. B. Corkum, A. Becker, and R. Dörner, Phys. Rev. Lett. **99**, 263002 (2007).

[28] A. Rudenko, V. L. B. de Jesus, T. Ergler, K. Zrost, B. Feuerstein, C. D. Schröter, R. Moshammer, and J. Ullrich, Phys. Rev. Lett. **99**, 263003 (2007).

[29] A. Emmanouilidou, J. S. Parker, L. R. Moore, and K. T. Taylor, New J. Phys. **13**, 043001 (2011).

[30] A. Chen, M. Kübel, B. Bergues, M. F. Kling, and A. Emmanouilidou, Sci. Rep. **7**, 7488 (2017).

[31] G. P. Katsoulis, A. Hadjipittas, B. Bergues, M. F. Kling, and A. Emmanouilidou, Phys. Rev. Lett. **121**, 263203 (2018).

[32] M. B. Peters, G. P. Katsoulis, and A. Emmanouilidou, Phys. Rev. A **105**, 043102 (2022).

[33] A. Emmanouilidou and T. Meltzer, Phys. Rev. A **95**, 033405 (2017).

[34] A. Emmanouilidou, T. Meltzer, and P. B. Corkum, J. Phys. B: At. Mol. Opt. Phys. **50**, 225602 (2017).

[35] L. D. Landau and E. M. Lifshitz, *Quantum Mechanics: Non-Relativistic Theory*, 2nd ed. (Pergamon, Oxford, UK, 1965).

[36] N. B. Delone and V. P. Krainov, J. Opt. Soc. Am. B **8**, 1207 (1991).

[37] See Supplemental Material at http://link.aps.org/supplemental/10.1103/PhysRevA.107.L041101 for the rate equations for single and sequential double ionization, for the Hamiltonian of the four-body system for the H model, for the criteria used to define an electron as quasifree or bound during time propagation, for the criteria used to identify the pathways of triple and double ionization, and for the correlated momenta.

[38] R. Y. Rubinstein and D. P. Froese, *Simulation and the Monte Carlo Method*, 3rd ed. (Wiley, Hoboken, NJ, 2016).

[39] B. HuP, J. Liu, and S.-G. Chen, Phys. Lett. A **236**, 533 (1997).

[40] N. B. Delone and V. P. Krainov, Phys.-Usp. **41**, 469 (1998).

[41] L. Fechner, N. Camus, J. Ullrich, T. Pfeifer, and R. Moshammer, Phys. Rev. Lett. **112**, 213001 (2014).

[42] V. J. Montemayor and G. Schiwietz, Phys. Rev. A **40**, 6223 (1989).

[43] L. Sarkadi, Phys. Rev. A **103**, 053113 (2021).

[44] J. G. Leopold and I. C. Percival, J. Phys. B: At., Mol. Phys. **12**, 709 (1979).